

# Imaging small numbers of Ba atoms in solid xenon for barium tagging in nEXO

T. Walton,<sup>1</sup> C. Chambers,<sup>1</sup> A. Craycraft,<sup>1</sup> W. Fairbank Jr.,<sup>1,\*</sup> J.B. Albert,<sup>2</sup> D.J. Auty,<sup>3</sup> P.S. Barbeau,<sup>4</sup>  
V. Basque,<sup>5</sup> D. Beck,<sup>6</sup> M. Breidenbach,<sup>7</sup> **T. Brunner,<sup>8</sup>** G.F. Cao,<sup>9</sup> B. Cleveland,<sup>10,†</sup> M. Coon,<sup>6</sup>  
T. Daniels,<sup>7</sup> S.J. Daugherty,<sup>2</sup> R. DeVoe,<sup>11</sup> T. Didberidze,<sup>3</sup> J. Dilling,<sup>12</sup> M.J. Dolinski,<sup>13</sup>  
M. Dunford,<sup>5</sup> L. Fabris,<sup>14</sup> J. Farine,<sup>10</sup> W. Feldmeier,<sup>15</sup> P. Fierlinger,<sup>15</sup> D. Fudenberg,<sup>11</sup>  
G. Giroux,<sup>16,‡</sup> R. Gornea,<sup>16</sup> K. Graham,<sup>5</sup> G. Gratta,<sup>11</sup> M. Heffner,<sup>17</sup> M. Hughes,<sup>3</sup> X.S. Jiang,<sup>9</sup>  
T.N. Johnson,<sup>2</sup> S. Johnston,<sup>18</sup> A. Karelina,<sup>19</sup> L.J. Kaufman,<sup>2</sup> R. Killick,<sup>5</sup> T. Koffas,<sup>5</sup> S. Kravitz,<sup>11</sup>  
R. Krücken,<sup>12</sup> A. Kuchenkov,<sup>19</sup> K.S. Kumar,<sup>20</sup> D.S. Leonard,<sup>21</sup> C. Licciardi,<sup>5</sup> Y.H. Lin,<sup>13</sup>  
J. Ling,<sup>6</sup> R. MacLellan,<sup>22</sup> M.G. Marino,<sup>15</sup> B. Mong,<sup>1,10</sup> D. Moore,<sup>11</sup> A. Odian,<sup>7</sup> I. Ostrovskiy,<sup>11</sup>  
A. Piepke,<sup>3</sup> A. Pocar,<sup>18</sup> F. Retiere,<sup>12</sup> P.C. Rowson,<sup>7</sup> M.P. Roza,<sup>5</sup> A. Schubert,<sup>11</sup> D. Sinclair,<sup>12,5</sup>  
E. Smith,<sup>13</sup> V. Stekhanov,<sup>19</sup> M. Tarka,<sup>6</sup> T. Tolba,<sup>16</sup> K. Twelker,<sup>11</sup> J.-L. Vuilleumier,<sup>16</sup>  
J. Walton,<sup>6</sup> M. Weber,<sup>11</sup> L.J. Wen,<sup>9</sup> U. Wichoski,<sup>10</sup> L. Yang,<sup>6</sup> Y.-R. Yen,<sup>13</sup> and Y.B. Zhao<sup>9</sup>

<sup>1</sup>*Physics Department, Colorado State University, Fort Collins CO, USA*

<sup>2</sup>*Physics Department and CEEM, Indiana University, Bloomington IN, USA*

<sup>3</sup>*Department of Physics and Astronomy, University of Alabama, Tuscaloosa AL, USA*

<sup>4</sup>*Department of Physics, Duke University, and Triangle Universities  
Nuclear Laboratory (TUNL), Durham North Carolina, USA*

<sup>5</sup>*Physics Department, Carleton University, Ottawa ON, Canada*

<sup>6</sup>*Physics Department, University of Illinois, Urbana-Champaign IL, USA*

<sup>7</sup>*SLAC National Accelerator Laboratory, Stanford CA, USA*

<sup>8</sup>***no longer at Physics Department, Stanford University, Stanford CA, USA others moved?***

<sup>9</sup>*Institute of High Energy Physics, Beijing, China*

<sup>10</sup>*Department of Physics, Laurentian University, Sudbury ON, Canada*

<sup>11</sup>*Physics Department, Stanford University, Stanford CA, USA*

<sup>12</sup>*TRIUMF, Vancouver BC, Canada*

<sup>13</sup>*Department of Physics, Drexel University, Philadelphia PA, USA*

<sup>14</sup>*Oak Ridge National Laboratory, Oak Ridge TN, USA*

<sup>15</sup>*Technische Universität München, Physikdepartment and Excellence Cluster Universe, Garching, Germany*

<sup>16</sup>*LHEP, Albert Einstein Center, University of Bern, Bern, Switzerland*

<sup>17</sup>*Lawrence Livermore National Laboratory, Livermore CA, USA*

<sup>18</sup>*Amherst Center for Fundamental Interactions and Physics Department,  
University of Massachusetts, Amherst MA, USA*

<sup>19</sup>*Institute for Theoretical and Experimental Physics, Moscow, Russia*

<sup>20</sup>*Department of Physics and Astronomy, Stony Brook University, SUNY, Stony Brook NY, USA*

<sup>21</sup>*Department of Physics, University of Seoul, Seoul, Korea*

<sup>22</sup>*Department of Physics, University of South Dakota, Vermillion SD, USA*

(Dated: August 21, 2015)

Images of Ba atoms in solid Xe in a focused laser region, after deposition from vacuum onto a cold sapphire window, are obtained using a 619-nm fluorescence peak down to the single-atom level. This is an important step toward barium tagging with a cryogenic probe from liquid Xe for the nEXO neutrinoless double beta decay experiment.

## I. INTRODUCTION

The search for neutrinoless double beta decay ( $0\nu\beta\beta$ ) is the most sensitive approach in determining the origin of neutrino mass, which is determined

non-zero by neutrino oscillations, but is not described by the standard model. Observation of  $0\nu\beta\beta$  would require that neutrinos are Majorana particles, which is integral to several favored standard model extensions [1], and would also violate conservation of lepton number, a yet only empirically conserved quantity. Additionally, measurement of the  $0\nu\beta\beta$  half-life would provide information needed to determine the effective mass of the electron neutrino  $\langle m_{\nu_e} \rangle$ .

EXO-200 is searching for  $0\nu\beta\beta$  in  $^{136}\text{Xe}$  with

\* Corresponding author

† Also SNOLAB, Sudbury ON, Canada

‡ Now at Queen's University, Kingston ON, Canada

110 kg of active liquid Xe (lXe) enriched to 80.6%  $^{136}\text{Xe}$  in a dual time projection chamber (TPC). The 3D event reconstruction of a TPC, as well as the separate collection of both scintillation and ionization signals, provide event discrimination beyond simple calorimetry, e.g. in distinguishing gamma events which Compton scatter one or more times in different locations in the detector. EXO-200 has measured the standard-model-allowed two-neutrino double beta decay ( $2\nu\beta\beta$ ) half-life of  $^{136}\text{Xe}$  at  $T_{1/2}^{2\nu\beta\beta} = 2.165 \pm 0.016(\text{stat}) \pm 0.059(\text{sys}) \times 10^{21}$  yr [2]. The most recent EXO-200  $0\nu\beta\beta$  search sets a limit on the half-life at  $T_{1/2}^{0\nu\beta\beta} < 1.1 \times 10^{25}$  yr (90% CL), which corresponds to  $\langle m_{\nu_e} \rangle < 190\text{--}450$  meV depending on nuclear matrix element calculations [3].

nEXO, the ton-scale successor to EXO-200, is now in the design stages. With a larger active mass of  $^{136}\text{Xe}$ , nEXO will probe Majorana neutrino masses through the entirety of the inverted hierarchy phase space, and into regions allowed only by the normal hierarchy.

But a lXe TPC also has a unique opportunity to tag the daughter at the site of a double beta decay event. Barium tagging would improve  $0\nu\beta\beta$  sensitivity by effectively eliminating all backgrounds [4]. It is hoped that nEXO will implement barium tagging in its second phase of operation. Techniques are under investigation for barium tagging in both liquid and gas time projection chambers (TPCs). The method described here is for barium tagging in the nEXO lXe TPC, in which a cryogenic probe would be moved to the position of the  $0\nu\beta\beta$  candidate in order to freeze the daughter ion into a small amount of solid Xe (sXe) at the end of the probe. It would then be detected by its laser-induced fluorescence in the sXe. Progress for another possible technique for barium tagging from lXe, using resonant ionization of the Ba after it is grabbed on a surface, is reported in [5]. *Mention hot probe? attempts at in situ and extracting from sXe?* Progress on a technique for extracting a single ion from a possible future Xe gas TPC and moving it to a trap for detection is described in [6].

It is expected that a  $\text{Ba}^{++}$  ion will neutralize once to  $\text{Ba}^+$  in lXe, as the lXe conduction band gap is slightly less than the ionization potential for  $\text{Ba}^+$  [4]. It is also not known whether the  $\text{Ba}^{++}$  might neutralize completely in the charge cloud following a  $\beta\beta$  event. A new study of neutralization of alpha decay daughters in the EXO-200 lXe TPC, is in the process of publication [ref? arxiv? example of arxiv ref in 2014 nu review, [185]]. Furthermore, a  $\text{Ba}^+$  ion may neutralize when it is grabbed in sXe in a cold

probe. As a result, the feasibility of detecting single Ba ions as well as atoms is still of interest. This work focuses on imaging single Ba atoms in sXe.

The spectroscopy of Ba in sXe is described in detail in the previous work [7]. Several emission peaks are observed and attributed to Ba atoms occupying different sites in the Xe matrix. In progression toward single-atom sensitivity, an image of  $\leq 10^4$  Ba atoms was obtained with the strong fluorescence peaks at 577 and 591 nm. However, bleaching of these fluorescence peaks with laser exposure was shown to reduce the 577- and 591-nm emission rapidly at high laser intensity, e.g., using a focused beam. It is possible that this bleaching is due to optical pumping of Ba into the metastable  $6s5d$  states in vacuum. Thus obtaining large numbers of photons from single Ba atoms is difficult without the use of infrared repumping lasers. However, the 619-nm emission peak has weaker bleaching by many orders of magnitude, and therefore is of interest for detecting single atoms.

## II. APPARATUS AND METHOD

The apparatus for depositing and observing Ba/Ba $^+$  deposits in sXe is described in [7]. Important components are shown in Fig. 1. The main source of  $\text{Ba}^+$  is an ion beam at 2000 eV, filtered to select  $\text{Ba}^+$  with an E $\times$ B velocity filter. A set of pulsing plates allows 1- $\mu\text{s}$  [I think we should say 1, because the analyzed pulse is just about 1  $\mu\text{s}$  long. It is probably lower than 1  $\mu\text{s}$  of DC due to spreading of the beam, since  $\text{Ba}^+$  is somewhat slow relative to the pulse time] pulses for depositing small numbers of ions. The spectra of  $\text{Ba}^+$  ion deposits in the sXe matrix exhibit peaks known to be due to neutral Ba atoms [7]. Thus some percentage of the ions neutralize in the matrix, but the fraction has not yet been determined. An alternative source of neutral Ba is a  $\text{BaAl}_4$  endothermic getter wire which can be inserted to emit toward the sample. However, it is challenging to achieve low Ba flux with this source and to calibrate it.

Deposits are made on a cold sapphire window tilted at  $45^\circ$ . To create a sample, Xe gas is directed toward the window using a leak valve, which begins freezing to form the sXe matrix. This is initiated a few seconds prior to the Ba deposit, continues during the Ba deposit, and is turned off a few seconds after the Ba deposit.

In this work, deposits are made with the sapphire window at around 50 K. This accomplishes (a) higher 619-nm signal, likely due to a higher popula-

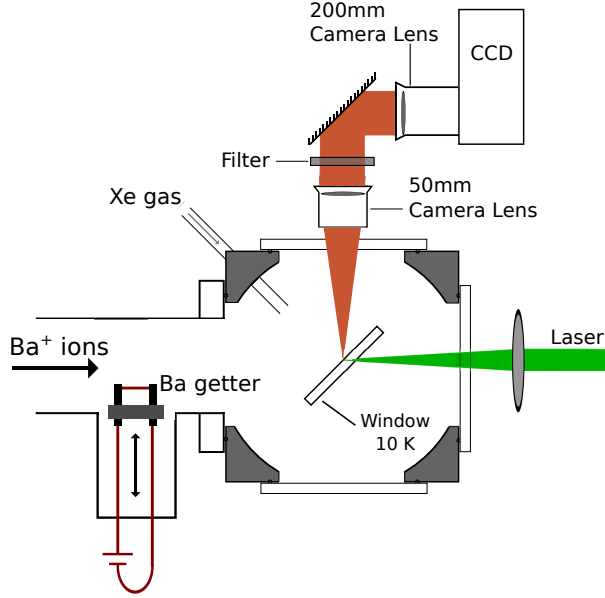


FIG. 1. Experimental setup for depositing Ba/Ba<sup>+</sup> in sXe matrices, and for excitation and observation. *want to put compensator in, and depict laser lens as asphere.*

tion of 619-nm matrix sites, and (b) a reduction of hydrogen in the matrix, as hydrogen freezes well below 50 K in vacuum [7]. The window is then cooled further to 11 K for observation. Xe deposition at around 50 nm/s also result in greater emission at 619 nm (as compared to lower leak rates), while not being so high as to result in a frosty Xe matrix. In an experiment, a deposit is made and observed, and then evaporated by heating the window to 100 K. Multiple deposits are made in a day with varying numbers of ions deposited, as well as periodic Xe-only deposits to keep track of the background.

The excitation laser, a Coherent 599 cw dye laser with Rhodamine 6G dye pumped by the 514-nm line of a Lexel 3500 argon ion laser, enters from the back side of the window. Ba fluorescence light is collected and collimated by a 50 mm Nikon camera lens. A band-pass filter with FWHM of 20 nm is in the collimated path passes just the 619-nm fluorescence peak. A 200 mm Nikon camera lens then focuses the image onto a liquid nitrogen cooled CCD, resulting in an image of 4x magnification. Each of the 20×20  $\mu\text{m}$  pixels of the CCD thus represents approximately 5×5  $\mu\text{m}$  on the SXe sample.

For a given laser intensity, the smallest focus possible is desired for reducing backgrounds in the single-atom signal. To achieve this, an optical flat is placed at 10° in the focusing region of the laser in order to compensate for astigmatism caused by the

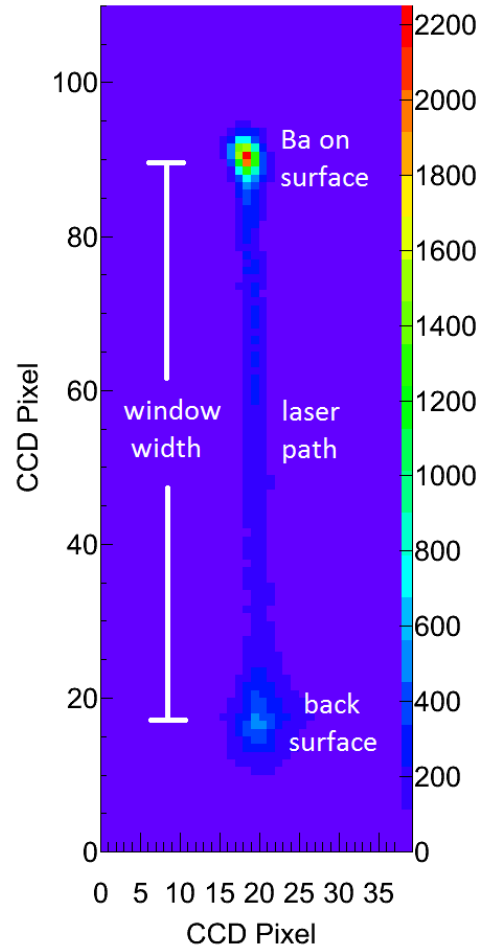


FIG. 2. Example image of Ba<sup>+</sup> deposit in focused laser. Pixels are 5  $\mu\text{m}$ ×5  $\mu\text{m}$ .

tilted sapphire window (see Fig. 1).

### III. RESULTS

A typical image made with a focused laser beam at 570 nm is shown in Fig. 2. The laser's path through the sapphire window is seen as a weak vertical line. At both ends, some background emission from the surfaces is observed. At the front surface (at the top in the image), extra fluorescence is detected from a small number of Ba atoms within the focused laser beam.

The number of Ba<sup>+</sup> ions deposited within the 1/e radius of the laser beam gives a rough upper limit to the number of Ba atoms responsible for the observed signal. For ion pulses of 13 fC/pulse and a focused

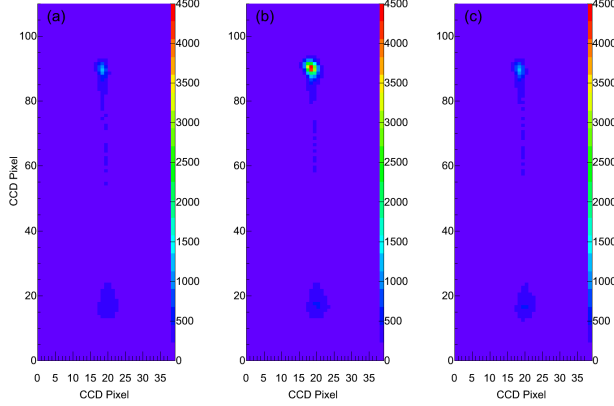


FIG. 3. Image of a 56-ion deposit with local sXe-only deposits: (a) sXe-only, (b)  $\leq 56$  atoms in sXe, (c) sXe-only. Pixels are  $5 \mu\text{m} \times 5 \mu\text{m}$ .

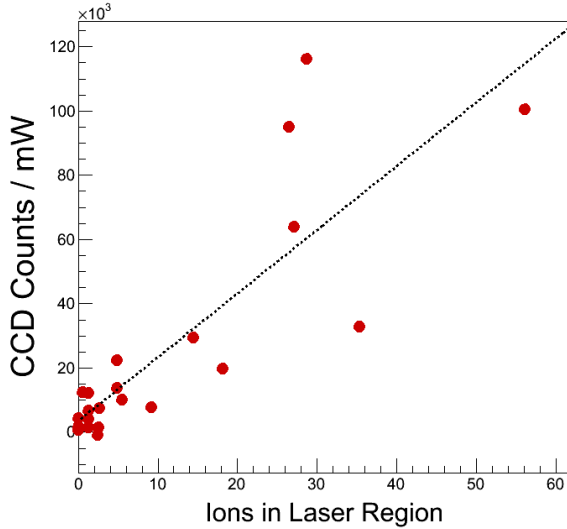


FIG. 4. 619-nm Ba fluorescence vs. number of ions deposited. *Could use better ion beam consistency.*

laser beam with  $1/e^2$  radius  $w = 2.1 \mu\text{m}$ , this results in about  $0.05 \text{ Ba}^+$  ions/pulse in the above area. The signal in Fig. 3 corresponds to a deposit of about  $14 \text{ Ba}^+$  ions into the laser region, and is therefore roughly due to  $\leq 14 \text{ Ba}$  atoms. A  $\leq 56$ -atom deposit (56 ions deposited) is shown in Fig. 3b, with Xe-only deposits made before and after (Fig. 3a,c)). It is important that no Ba is left over after evaporating the sample, even for larger deposits.

The counts vs. ions deposited are plotted in Fig. 4. Observe the linearity in summed CCD counts, from the image of the laser region in the

sXe, vs. ions deposited for several deposits. Each point has subtracted the counts from a nearby Xe-only run. The observed signal corresponds to about 2000 counts/mW per atom with 60-s CCD exposures. Counts are scaled by laser power to account for small variations in laser power.

To obtain images of Ba fluorescence, sXe-only images are subtracted [This isn't said in explanation of linearity plot because those do not directly subtract images, they subtract integrated counts after using integration regions specific to each run (due to slight movements)]. A subtracted image of a deposit corresponding to a single Ba atom is shown in Fig. 5. A solitary peak is observed from the Ba in the laser region.

A Gaussian fit to the images gives a  $1/e^2$  radius of about  $12 \mu\text{m}$ , which is much larger than the laser beam radius of  $w = 2.1 \mu\text{m}$ . Aberrations and vibrations in the collection optics and imperfections in the surface of the sXe layer could contribute to blurring of the image. Relative motion of the laser and the window could also lead to image broadening and to exposure of more Ba atoms than calculated above. *The latter effect has been checked by observing images of the focused laser relative to a reference point on the sapphire window on time frames down to 50 ms. Maximum vibrations observed were on the order of  $2 \mu\text{m}$ .*

#### A. Scanned Images

*Put scanned image of single atoms here.*

#### B. Identification of 619-nm Peak as Ba in sXe

Deposits made with the neutral Ba getter source are compared to a  $\text{Ba}^+$  deposit in Fig. 6. Identical spectra are observed using the different sources under similar deposit conditions, confirming the identification of neutral Ba. Another peak at 670 nm which is mentioned in [7] is also attributed to Ba, likely in another Xe matrix site. Observing Ba in the 619-nm matrix site at the low-energy (thermal) deposit from the getter is also good news for the prospect of grabbing  $\text{Ba}/\text{Ba}^+$  on a probe out of lXe.

An absence of fluorescence is observed from deposits of  $\text{Ar}^+$  in sXe (Fig. 6).  $\text{Ar}^+$  ions are deposited with the same ion beam, also at 2000 eV, and under the same conditions. This further rules out any matrix-damage-related sources of the 619-nm peak, such as fluorescent color centers.

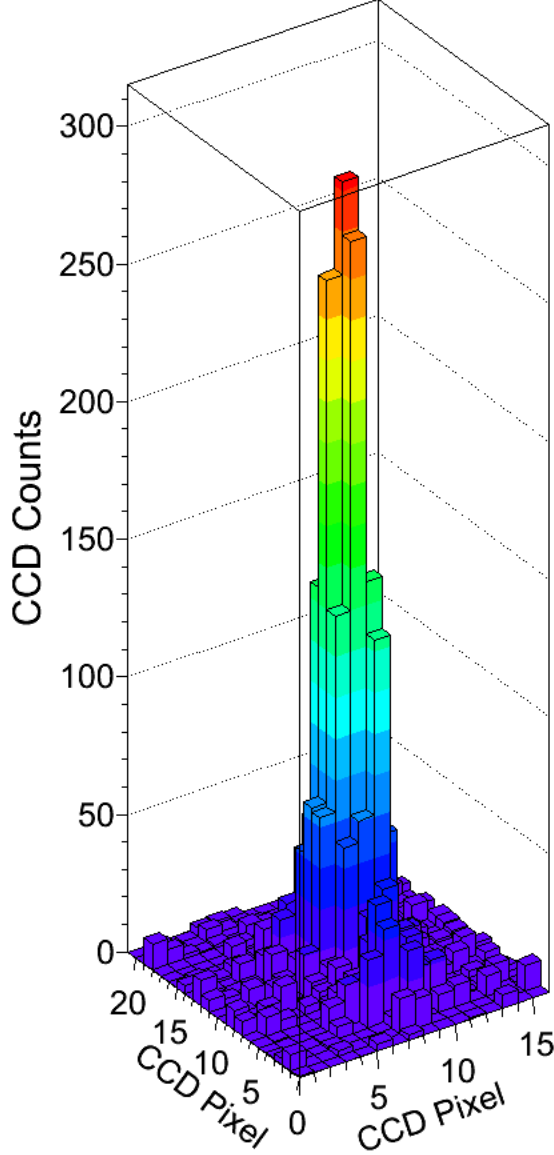


FIG. 5. Image of a single Ba atom in a focused  $w = 2.1 \mu\text{m}$  laser beam, with 60 s exposure of 0.18 mW laser power.

### C. Backgrounds

Very low concentrations of  $\text{Cr}^{3+}$  in the sapphire bulk (sub-ppb level) produce a broad fluorescence, the tail of which enters the 610-630 nm region passed by the band-pass filter and produces the faintly visible line through the sapphire window discussed above. This fluorescence is identified as  $\text{Cr}^{3+}$  by its

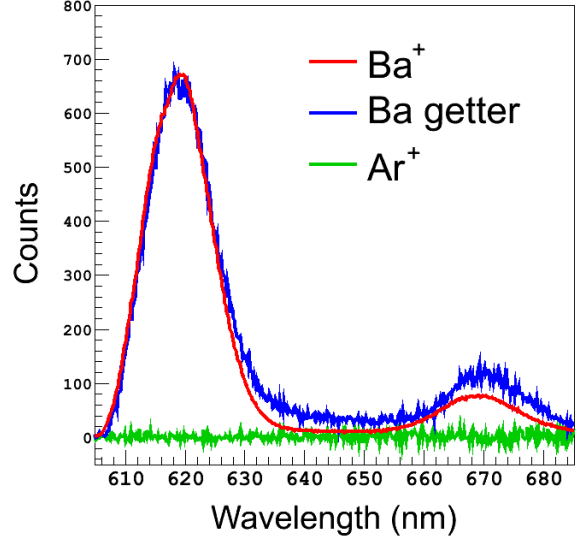


FIG. 6. Observation of deposits from three different sources in sXe. Curves are scaled due to different deposit sizes.

excitation spectrum, identical to that of the well-known lines around 693 nm. *Show figure?* Commercially available c-plane quality sapphire (*mention Meller?*) has sufficiently low concentrations for the 619-nm single atom signal level.

Another background is observed on the surfaces of the window, also caused by laser excitation. This is more of a nuisance, as it not as easily distinguished from the Ba in an image. It also exhibits bleaching, which can cause confusion in subtractions, though its bleaching rate is different from that of the 619-nm Ba emission. (*Mention temp.-dependence?*) To minimize this, the window is exposed to the laser until the background reaches a steady value. The set of deposits used for Fig. 4 was done after about an hour of pre-exposure of the sapphire window to the focused laser.

*Do we want a bleaching section?*

## IV. CONCLUSIONS

The 619-nm emission peak observed in deposits of  $\text{Ba}^+$  and Ba in sXe is attributed to neutral Ba *in a stable and relatively abundant matrix site*. Images of 619-nm fluorescence in a focused laser region from Ba atoms are achieved down to an average number of Ba atoms at the single-atom level. Successful detection of Ba atoms in sXe at this level is a significant

step toward Ba tagging technique in nEXO.

## ACKNOWLEDGEMENTS

Shon Cook and Brian Mong for pioneering work and primary authorship in [7]. This material is based upon work supported by the National Science Foundation under Grant Number PHY-1132428 and the U.S. Department of Energy, Office of Science, Office of High Energy Physics **under Award Number DE-FG02-03ER41255.**

- 
- [1] K.A. Olive *et al.* (Particle Data Group), “14. Neutrino Mass, Mixing, and Oscillations,” *Chin. Phys. C* **38**, 090001 (2014) (<http://pdg.lbl.gov>).
  - [2] J. Albert *et al.* (EXO-200 Collaboration), *Phys. Rev. C* **89**, 015502 (2014).
  - [3] J. Albert *et al.* (EXO-200 Collaboration), *Nature* **510**, 229 (2014).
  - [4] M. Moe, *Phys. Rev. C* **44**, R931 (1991).
  - [5] K. Twelker *et al.*, *Review of Scientific Instruments* **85**, 095114 (2014).
  - [6] T. Brunner *et al.*, *International Journal of Mass Spectrometry* **379** (2015) 110-120.
  - [7] B. Mong *et al.*, *Phys. Rev. A* **91**, 022505 (1954).